i.e. there is a simple trade off between beam dimension and divergence.

The second type of capillary optic is a monolithic configuration. The individual capillaries in monolithic optics are tapered and fused together, so that no external frame assembly is necessary (Chen-Mayer *et al.*, 1996). Unlike the multifibre devices, the inner diameters of the channels that make up the monolithic optics vary along the length of the component, resulting in a smaller more compact design.

Further applications of capillary optics include small-angle scattering (Mildner, 1994) and lenses for high-spatial-resolution area detection.

4.4.2.5. *Filters*

Neutron filters are used to remove unwanted radiation from the beam while maintaining as high a transmission as possible for the neutrons of the required energy. Two major applications can be identified: removal of fast neutrons and γ-rays from the primary beam and reduction of higher-order contributions (λ/n) in the secondary beam reflected from crystal monochromators. In this section, we deal with non-polarizing filters, *i.e.* those whose transmission and removal cross sections are independent of the neutron spin. Polarizing filters are discussed in the section concerning polarizers.

Filters rely on a strong variation of the neutron cross section with energy, usually either the wavelength-dependent scattering cross section of polycrystals or a resonant absorption cross section. Following Freund (1983), the total cross section determining the attenuation of neutrons by a crystalline solid can be written as a sum of three terms,

$$\sigma = \sigma_{\rm abs} + \sigma_{\rm tds} + \sigma_{\rm Bragg}. \qquad (4.4.2.7)$$

Here, $\sigma_{\rm abs}$ is the true absorption cross section, which, at low energy, away from resonances, is proportional to $E^{-1/2}$. The temperature-dependent thermal diffuse cross section, $\sigma_{\rm tds}$, describing the attenuation due to inelastic processes, can be split into two parts depending on the neutron energy. At low energy, $E \ll k_b\Theta_D$, where k_b is Boltzmann's constant and Θ_D is the characteristic Debye temperature, single-phonon processes dominate, giving rise to a cross section, $\sigma_{\rm sph}$, which is also proportional to $E^{-1/2}$. The single-phonon cross section is proportional to $T^{7/2}$ at low temperatures and to T at higher temperatures. At higher energies, $E \geq k_b\Theta_D$, multiphonon and multiple-scattering processes come into play, leading to a cross section, $\sigma_{\rm mph}$, that increases with energy and temperature. The third contribution, $\sigma_{\rm Bragg}$, arises due to Bragg scattering in single- or polycrystalline material. At low energies, below the Bragg cut-off ($\lambda > 2d_{\rm max}$), $\sigma_{\rm Bragg}$ is zero. In polycrystalline materials, the cross section rises steeply above the Bragg cut-off and oscillates with increasing energy as more reflections come into play. At still higher energies, $\sigma_{\rm Bragg}$ decreases to zero.

In single-crystalline material above the Bragg cut-off, $\sigma_{\rm Bragg}$ is characterized by a discrete spectrum of peaks whose heights and widths depend on the beam collimation, energy resolution, and the perfection and orientation of the crystal. Hence a monocrystalline filter has to be tuned by careful orientation.

The resulting attenuation cross section for beryllium is shown in Fig. 4.4.2.7. Cooled polycrystalline beryllium is frequently used as a filter for neutrons with energies less than 5 meV, since there is an increase of nearly two orders of magnitude in the attenuation cross section for higher energies. BeO, with a Bragg cut-off at approximately 4 meV, is also commonly used.

Pyrolytic graphite, being a layered material with good crystalline properties along the c direction but random orientation perpendicular to it, lies somewhere between a polycrystal and a single crystal as far as its attenuation cross section is concerned. The energy-dependent cross section for a neutron beam incident along the c axis of a pyrolytic graphite filter is shown in Fig. 4.4.2.8, where the attenuation peaks due to the 00ξ reflections can be seen. Pyrolytic graphite serves as an efficient second- or third-order filter (Shapiro & Chesser, 1972) and can be 'tuned' by slight misorientation away from the c axis.

Further examples of typical filter materials (*e.g.* silicon, lead, bismuth, sapphire) can be found in the paper by Freund (1983).

Resonant absorption filters show a large increase in their attenuation cross sections at the resonant energy and are therefore used as selective filters for that energy. A list of typical filter materials and their resonance energies is given in Table 4.4.2.3.

4.4.2.6. *Polarizers*

Methods used to polarize a neutron beam are many and varied, and the choice of the best technique depends on the instrument and the experiment to be performed. The main parameter that has to be considered when describing the effectiveness of a given polarizer is the polarizing efficiency, defined as

$$P = (N_+ - N_-)/(N_+ + N_-), \qquad (4.4.2.8)$$

where N_+ and N_- are the numbers of neutrons with spin parallel (+) or antiparallel (−) to the guide field in the outgoing beam. The second important factor, the transmission of the wanted spin state, depends on various factors, such as acceptance angles, reflection, and absorption.

4.4.2.6.1. *Single-crystal polarizers*

The principle by which ferromagnetic single crystals are used to polarize and monochromate a neutron beam simultaneously is shown in Fig. 4.4.2.9. A field **B**, applied perpendicular to the scattering vector $\boldsymbol{\kappa}$, saturates the atomic moments $\mathbf{M}_\nu$ along the field direction. The cross section for Bragg reflection in this geometry is

$$(\mathrm{d}\sigma/\mathrm{d}\Omega) = F_N(\boldsymbol{\kappa})^2 + 2F_N(\boldsymbol{\kappa})F_M(\boldsymbol{\kappa})(\mathbf{P}\cdot\boldsymbol{\mu}) + F_M(\boldsymbol{\kappa})^2, \quad (4.4.2.9)$$

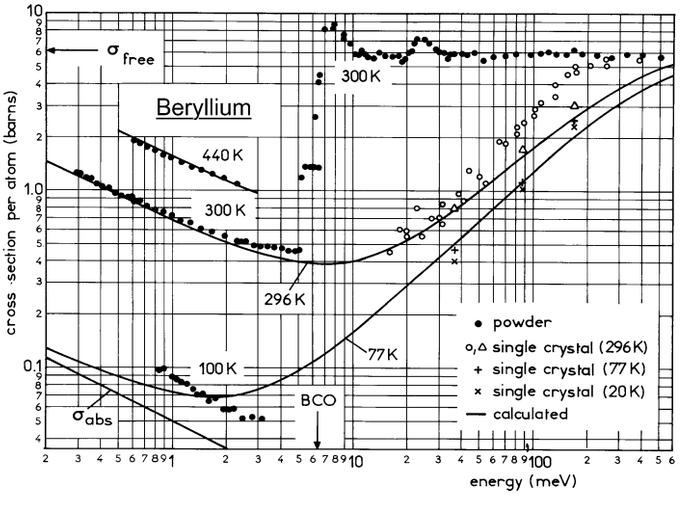

Fig. 4.4.2.7. Total cross section for beryllium in the energy range where it can be used as a filter for neutrons with energy below 5 meV (Freund, 1983).

Table 4.4.2.3. *Characteristics of some typical elements and isotopes used as neutron filters*

Element or isotope	Resonance (eV)	σ_s (resonance) (barns)	λ (Å)	$\sigma_s(\lambda)$ (barns)	$\frac{\sigma_s(\lambda/2)}{\sigma_s(\lambda)}$
In	1.45	30000	0.48	94	319
Rh	1.27	4500	0.51	76	59.2
Hf	1.10	5000	0.55	58	86.2
^{240}Pu	1.06	115000	9.55	145	793
Ir	0.66	4950	0.70	183	27.0
^{229}Th	0.61	6200	0.73	<100	>62.0
Er	0.58	1500	0.75	127	11.8
Er	0.46	2300	0.84	125	18.4
Eu	0.46	10100	0.84	1050	9.6
^{231}Pa	0.39	4900	0.92	116	42.2
^{239}Pu	0.29	5200	1.06	700	7.4

1 barn $= 10^{-28}$ m^2.

where $F_N(\boldsymbol{\kappa})$ is the nuclear structure factor and $F_M(\boldsymbol{\kappa}) = [(\gamma/2)r_0] \sum_\nu M_\nu f(hkl) \exp[2\pi(hx + ky + lz)]$ is the magnetic structure factor, with $f(hkl)$ the magnetic form factor of the magnetic atom at the position (x, y, z) in the unit cell. The vector $\mathbf{P}$ describes the polarization of the incoming neutron with respect to $\mathbf{B}$; $\mathbf{P} = 1$ for $+$ spins and $\mathbf{P} = -1$ for $-$ spins and $\boldsymbol{\mu}$ is a unit vector in the direction of the atomic magnetic moments. Hence, for neutrons polarized parallel to $\mathbf{B}$ $(\mathbf{P} \cdot \boldsymbol{\mu} = 1)$, the diffracted intensity is proportional to $[F_N(\boldsymbol{\kappa}) + F_M(\boldsymbol{\kappa})]^2$, while, for neutrons polarized antiparallel to $\mathbf{B}$ $(\mathbf{P} \cdot \boldsymbol{\mu} = -1)$, the diffracted intensity is proportional to $[F_N(\boldsymbol{\kappa}) - F_M(\boldsymbol{\kappa})]^2$. The polarizing efficiency of the diffracted beam is then

$$P = \pm 2F_N(\boldsymbol{\kappa})F_M(\boldsymbol{\kappa})/[F_N(\boldsymbol{\kappa})^2 + F_M(\boldsymbol{\kappa})^2], \qquad (4.4.2.10)$$

which can be either positive or negative and has a maximum value for $|F_N(\boldsymbol{\kappa})| = |F_M(\boldsymbol{\kappa})|$. Thus, a good single-crystal polarizer, in addition to possessing a crystallographic structure in which F_N and F_M are matched, must be ferromagnetic at room temperature and should contain atoms with large magnetic moments. Furthermore, large single crystals with 'controllable' mosaic should be available. Finally, the structure factor for the required reflection should be high, while those for higher-order reflections should be low.

None of the three naturally occurring ferromagnetic elements (iron, cobalt, nickel) makes efficient single-crystal polarizers. Cobalt is strongly absorbing and the nuclear scattering lengths of iron and nickel are too large to be balanced by their weak magnetic moments. An exception is ^{57}Fe, which has a rather low nuclear scattering length, and structure-factor matching can be achieved by mixing ^{57}Fe with Fe and 3% Si (Reed, Bolling & Harmon, 1973).

In general, in order to facilitate structure-factor matching, alloys rather than elements are used. The characteristics of some alloys used as polarizing monochromators are presented in Table 4.4.2.4. At short wavelengths, the 200 reflection of $Co_{0.92}Fe_{0.08}$ is used to give a positively polarized beam [$F_N(\boldsymbol{\kappa})$ and $F_M(\boldsymbol{\kappa})$ both positive], but the absorption due to cobalt is high. At longer wavelengths, the 111 reflection of the Heusler alloy Cu_2MnAl (Delapalme, Schweizer, Couderchon & Perrier de la Bathie, 1971; Freund, Pynn, Stirling & Zeyen, 1983) is commonly used, since it has a higher reflectivity and a larger d spacing than $Co_{0.92}Fe_{0.08}$. Since for the 111 reflection $F_N \approx -F_M$, the diffracted beam is negatively polarized. Unfortunately, the structure factor of the 222 reflection is higher than that of the 111 reflection, leading to significant higher-order contamination of the beam.

Other alloys that have been proposed as neutron polarizers are $Fe_{3-x}Mn_xSi$, $^7Li_{0.5}Fe_{2.5}O_4$ (Bednarski, Dobrzynski & Steinsvoll, 1980), Fe_3Si (Hines *et al.*, 1976), Fe_3Al (Pickart & Nathans, 1961), and $HoFe_2$ (Freund & Forsyth, 1979).

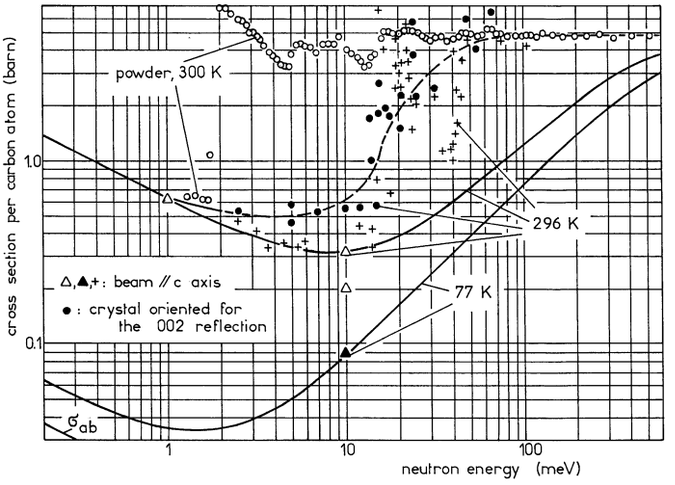

Fig. 4.4.2.8. Energy-dependent cross section for a neutron beam incident along the c axis of a pyrolytic graphite filter. The attenuation peaks due to the 00ξ reflections can be seen.

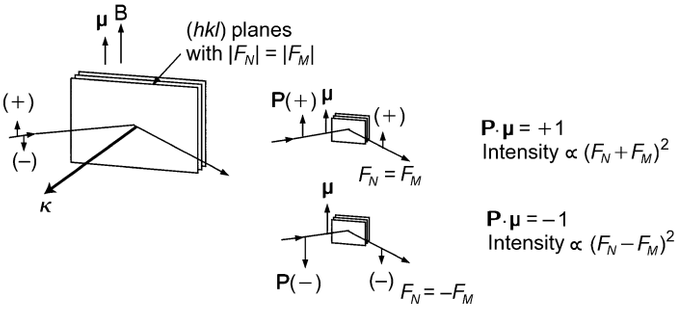

Fig. 4.4.2.9. Geometry of a polarizing monochromator showing the lattice planes (hkl) with $|F_N| = |F_M|$, the direction of $\mathbf{P}$ and $\boldsymbol{\mu}$, the expected spin direction and intensity.

Table 4.4.2.4. *Properties of polarizing crystal monochromators (Williams, 1988)*

	$Co_{0.92}Fe_{0.08}$	Cu_2MnAl	Fe_3Si	^{57}Fe:Fe	$HoFe_2$
Matched reflection $\|F_N\| \sim \|F_M\|$	200	111	111	110	620
d spacing (Å)	1.76	3.43	3.27	2.03	1.16
Take-off angle $2\theta_B$ at 1Å (°)	33.1	16.7	17.6	28.6	50.9
Cut-off wavelength, λ_{max} (Å)	3.5	6.9	6.5	4.1	2.3

4.4.2.6.2. *Polarizing mirrors*

For a ferromagnetic material, the neutron refractive index is given by

$$n_{\pm}^2 = 1 - \lambda^2 N(b_{coh} \pm p)/\pi, \qquad (4.4.2.11)$$

where the magnetic scattering length, p, is defined by

$$p = 2\mu(B - H)m\pi/h^2N. \qquad (4.4.2.12)$$

Here, m and μ are the neutron mass and magnetic moment, B is the magnetic induction in an applied field H, and h is Planck's constant.

The $-$ and $+$ signs refer, respectively, to neutrons whose moments are aligned parallel and antiparallel to B. The refractive index depends on the orientation of the neutron spin with respect to the film magnetization, thus giving rise to two critical angles of total reflection, γ_- and γ_+. Thus, reflection in an angular range between these two critical angles gives rise to polarized beams in reflection and in transmission. The polarization efficiency, P, is defined in terms of the reflectivity r_+ and r_- of the two spin states,

$$P = (r_+ - r_-)/(r_+ + r_-). \qquad (4.4.2.13)$$

The first polarizers using this principle were simple cobalt mirrors (Hughes & Burgy, 1950), while Schaerpf (1975) used FeCo sheets to build a polarizing guide. It is more common these days to use thin films of ferromagnetic material deposited onto a substrate of low surface roughness (*e.g.* float glass or polished silicon). In this case, the reflection from the substrate can be eliminated by including an antireflecting layer made from, for example, Gd–Ti alloys (Drabkin *et al.*, 1976). The major limitation of these polarizers is that grazing-incidence angles must be used and the angular range of polarization is small. This limitation can be partially overcome by using multilayers, as described above, in which one of the layer materials is ferromagnetic. In this case, the refractive index of the ferromagnetic material is matched for one spin state to that of the non-magnetic material, so that reflection does not occur. A polarizing supermirror made in this way has an extended angular range of polarization, as indicated in Fig. 4.4.2.10. It should be noted that modern deposition techniques allow the refractive index to be adjusted readily, so that matching is easily achieved. The scattering-length densities of some commonly used layer pairs are given in Table 4.4.2.5

Polarizing multilayers are also used in monochromators and broad-band devices. Depending on the application, various layer pairs have been used: Co/Ti, Fe/Ag, Fe/Si, Fe/Ge, Fe/W, FeCoV/TiN, FeCoV/TiZr, $^{63}Ni_{0.66}{}^{54}Fe_{0.34}$/V and the range of fields used to achieve saturation varies from about 100 to 500 Gs.

Polarizing mirrors can be used in reflection or transmission with polarization efficiencies reaching 97%, although, owing to the low incidence angles, their use is generally restricted to wavelengths above 2 Å.

Various devices have been constructed that use mirror polarizers, including simple reflecting mirrors, V-shaped transmission polarizers (Majkrzak, Nunez, Copley, Ankner & Greene, 1992), cavity polarizers (Mezei, 1988), and benders (Hayter, Penfold & Williams, 1978; Schaerpf, 1989). Perhaps the best known device is the polarizing bender developed by Schärpf. The device consists of 0.2 mm thick glass blades coated on both sides with a Co/Ti supermirror on top of an antireflecting Gd/Ti coating designed to reduce the scattering of the unwanted spin state from the substrate to a very low Q value. The device is quite compact (typically 30 cm long for a beam cross section up to 6×5 cm) and transmits over 40% of an unpolarized beam with the collimation from a nickel-coated guide for wavelengths above 4.5 Å. Polarization efficiencies of over 96% can be achieved with these benders.

4.4.2.6.3. *Polarizing filters*

Polarizing filters operate by selectively removing one of the neutron spin states from an incident beam, allowing the other spin state to be transmitted with only moderate attenuation. The spin selection is obtained by preferential absorption or scattering, so the polarizing efficiency usually increases with the thickness of the filter, whereas the transmission decreases. A compromise must therefore be made between polarization, P, and transmission, T. The 'quality factor' often used is $P\sqrt{T}$ (Tasset & Resouche, 1995).

The total cross sections for a generalized filter may be written as

$$\sigma_{\pm} = \sigma_0 \pm \sigma_p, \qquad (4.4.2.14)$$

where σ_0 is a spin-independent cross section and $\sigma_p = (\sigma_+ + \sigma_-)/2$ is the polarization cross section. It can be

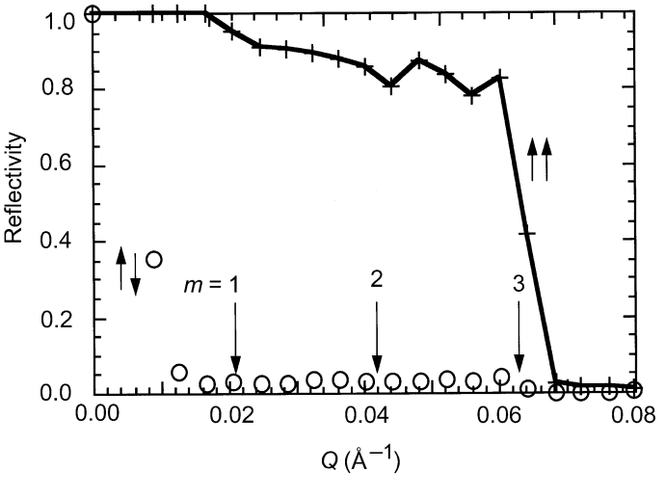

Fig. 4.4.2.10. Measured reflectivity curve of an FeCoV/TiZr polarizing supermirror with an extended angular range of polarization of three times that of γ_c(Ni) for neutrons without spin flip, ↑↑, and with spin flip, ↑↓.

Table 4.4.2.5. *Scattering-length densities for some typical materials used for polarizing multilayers*

Magnetic layer	$N(b+p)$ (10^{-6} Å^{-2})	$N(b-p)$ (10^{-6} Å^{-2})	Nb (10^{-6} Å^{-2})	Nonmagnetic layer
Fe	13.04	3.08	3.64	Ge
			3.50	Ag
			3.02	W
			2.08	Si
			2.08	Al
Fe:Co (50:50)	10.98	−0.52	−0.27	V
			−1.95	Ti
Ni	10.86	7.94		
Fe:Co:V (49:49:2)	10.75	−0.63	−0.27	V
			−1.95	Ti
Fe:Co:V (50:48:2)	10.66	−0.64	−0.27	V
			−1.95	Ti
Fe:Ni (50:50)	10.53	6.65		
Co	6.65	−2.00	−1.95	Ti
Fe:Co:V (52:38:10)	6.27	2.12	2.08	Si
			2.08	Al

For the non-magnetic layer we have only listed the simple elements that give a close match to the $N(b-p)$ value of the corresponding magnetic layer. In practice excellent matching can be achieved by using alloys (*e.g.* Ti_xZr_y alloys allow Nb values between −1.95 and 3.03×10^{-6}Å^{-2} to be selected) or reactive sputtering (*e.g.*TiN_x).

shown (Williams, 1988) that the ratio σ_p/σ_0 must be ≥ 0.65 to achieve $|P| > 0.95$ and $T > 0.2$.

Magnetized iron was the first polarizing filter to be used (Alvarez & Bloch, 1940). The method relies on the spin-dependent Bragg scattering from a magnetized polycrystalline block, for which σ_p approaches 10 barns near the Fe cut-off at 4 Å (Steinberger & Wick, 1949). Thus, for wavelengths in the range 3.6 to 4 Å, the ratio $\sigma_p/\sigma_0 \simeq 0.59$, resulting in a theoretical polarizing efficiency of 0.8 for a transmittance of ~ 0.3. In practice, however, since iron cannot be fully saturated, depolarization occurs, and values of $P \simeq 0.5$ with $T \sim 0.25$ are more typical.

Resonance absorption polarization filters rely on the spin dependence of the absorption cross section of polarized nuclei at their nuclear resonance energy and can produce efficient polarization over a wide energy range. The nuclear polarization is normally achieved by cooling in a magnetic field, and filters based on ^{149}Sm ($E_r = 0.097$ eV) (Freeman & Williams, 1978) and ^{151}Eu ($E_r = 0.32$ and 0.46 eV) have been successfully tested. The ^{149}Sm filter has a polarizing efficiency close to 1 within a small wavelength range (0.85 to 1.1 Å), while the transmittance is about 0.15. Furthermore, since the filter must be operated at temperatures of the order of 15 mK, it is very sensitive to heating by γ-rays.

Broad-band polarizing filters, based on spin-dependent scattering or absorption, provide an interesting alternative to polarizing mirrors or monochromators, owing to the wider range of energy and scattering angle that can be accepted. The most promising such filter is polarized ^{3}He, which operates through the huge spin-dependent neutron capture cross section that is totally dominated by the resonance capture of neutrons with antiparallel spin. The polarization efficiency of an ^{3}He neutron spin filter of length l can be written as

$$P_n(\lambda) = \tanh[\mathcal{O}(\lambda)P_{\rm He}], \qquad (4.4.2.15)$$

where $P_{\rm He}$ is the ^{3}He polarization, and $\mathcal{O}(\lambda) = [^3\mathrm{He}]l\sigma_0(\lambda)$ is the dimensionless effective absorption coefficient, also called the opacity (Surkau *et al.*, 1997). For gaseous ^{3}He, the opacity can be written in more convenient units as

$$\mathcal{O}' = p[\mathrm{bar}] \times l[\mathrm{cm}] \times \lambda[\text{Å}], \qquad (4.4.2.16)$$

where p is the ^{3}He pressure (1 bar = 10^5 Pa) and $\mathcal{O} = 7.33 \times 10^{-2}\mathcal{O}'$. Similarly, the residual transmission of the spin filter is given by

$$T_n(\lambda) = \exp[-\mathcal{O}(\lambda)]\cosh[\mathcal{O}(\lambda)P_{\rm He}]. \qquad (4.4.2.17)$$

It can be seen that, even at low ^{3}He polarization, full neutron polarization can be achieved in the limit of large absorption at the cost of the transmission.

^{3}He can be polarized either by spin exchange with optically pumped rubidium (Bouchiat, Carver & Varnum, 1960; Chupp, Coulter, Hwang, Smith & Welsh, 1996; Wagshul & Chupp, 1994) or by pumping of metastable ^{3}He* atoms followed by metastable exchange collisions (Colegrove, Schearer & Walters, 1963). In the former method, the ^{3}He gas is polarized at the required high pressure, whereas ^{3}He* pumping takes place at a pressure of about 1 mbar, followed by a polarization conserving compression by a factor of nearly 10 000. Although the polarization time constant for Rb pumping is of the order of several hours compared with fractions of a second for ^{3}He* pumping, the latter requires several 'fills' of the filter cell to achieve the required pressure.

An alternative broad-band spin filter is the polarized proton filter, which utilizes the spin dependence of nuclear scattering. The spin-dependent cross section can be written as (Lushchikov, Taran & Shapiro, 1969)

$$\sigma_\pm = \sigma_1 + \sigma_2 P_{\rm H}^2 \mp \sigma_3 P_{\rm H}, \qquad (4.4.2.18)$$

where σ_1, σ_2, and σ_3 are empirical constants. The viability of the method relies on achieving a high nuclear polarization $P_{\rm H}$. A polarization $P_{\rm H} = 0.7$ gives $\sigma_p/\sigma_0 \approx 0.56$ in the cold-neutron region. Proton polarizations of the order of 0.8 are required for a useful filter (Schaerpf & Stuesser, 1989). Polarized proton filters can polarize very high energy neutrons even in the eV range.

4.4.2.6.4. *Zeeman polarizer*

The reflection width of perfect silicon crystals for thermal neutrons and the Zeeman splitting ($\Delta E = 2\mu B$) of a field of about 10 kGs are comparable and therefore can be used to polarize a neutron beam. For a monochromatic beam (energy E_0) in a strong magnetic field region, the result of the Zeeman splitting will be a separation into two polarized subbeams, one polarized along **B** with energy $E_0 + \mu B$, and the other polarized antiparallel to **B** with energy $E_0 - \mu B$. The two polarized beams can be selected by rocking a perfect crystal in the field region B (Forte & Zeyen, 1989).

4.4.2.7. *Spin-orientation devices*

Polarization is the state of spin orientation of an assembly of particles in a target or beam. The beam polarization vector **P** is defined as the vector average of this spin state and is often described by the density matrix $\rho = \frac{1}{2}(1 + \sigma\mathbf{P})$. The polarization is then defined as $\mathbf{P} = \mathrm{Tr}(\rho\sigma)$. If the polarization vector is inclined to the field direction in a homogenous magnetic field, **B**, the polarization vector will precess with the classical Larmor frequency $\omega_L = |\gamma|B$. This results in a precessing spin polarization. For most experiments, it is sufficient to consider the linear polarization vector in the direction of an applied magnetic field. If, however, the magnetic field direction changes along the path of the neutron, it is also possible that the direction of **P** will change. If the frequency, Ω, with which the magnetic field changes is such that

$$\Omega = \mathrm{d}(\mathbf{B}/|\mathbf{B}|)/\,\mathrm{d}t \ll \omega_L, \qquad (4.4.2.19)$$

then the polarization vector follows the field rotation adiabatically. Alternatively, when $\Omega \gg \omega_L$, the magnetic field changes so rapidly that **P** cannot follow, and the condition is known as non-adiabatic fast passage. All spin-orientation devices are based on these concepts.

4.4.2.7.1. *Maintaining the direction of polarization*

A polarized beam will tend to become depolarized during passage through a region of zero field, since the field direction is ill defined over the beam cross section. Thus, in order to keep the polarization direction aligned along a defined quantization axis, special precautions must be taken.

The simplest way of maintaining the polarization of neutrons is to use a guide field to produce a well defined field **B** over the whole flight path of the beam. If the field changes direction, it has to fulfil the adiabatic condition $\Omega \ll \omega_L$, *i.e.* the field changes must take place over a time interval that is long compared with the Larmor period. In this case, the polarization follows the field direction adiabatically with an angle of deviation $\Delta\theta \leq 2\arctan(\Omega/\omega_L)$ (Schärpf, 1980).

Alternatively, some instruments (*e.g.* zero-field spin-echo spectrometers and polarimeters) use polarized neutron beams in regions of zero field. The spin orientation remains constant in a zero-field region, but the passage of the neutron beam into and out of the zero-field region must be well controlled. In order to provide a well defined region of transition from a guide-field region to a zero-field region, a non-adiabatic fast passage through the windings of a rectangular input solenoid can be used, either with a toroidal closure of the outside field or with a μ-metal closure frame. The latter serves as a mirror for the coil ends, with the effect of producing the field homogeneity of a long coil but avoiding the field divergence at the end of the coil.

4.4.2.7.2. *Rotation of the polarization direction*

The polarization direction can be changed by the adiabatic change of the guide-field direction so that the direction of the polarization follows it. Such a rotation is performed by a spin turner or spin rotator (Schärpf & Capellmann, 1993; Williams, 1988).

Alternatively, the direction of polarization can be rotated relative to the guide field by using the property of precession described above. If a polarized beam enters a region where the field is inclined to the polarization axis, then the polarization vector **P** will precess about the new field direction. The precession angle will depend on the magnitude of the field and the time spent in the field region. By adjustment of these two parameters together with the field direction, a defined, though wavelength-dependent, rotation of **P** can be achieved. A simple device uses the non-adiabatic fast passage through the windings of two rectangular solenoids, wound orthogonally one on top of the other. In this way, the direction of the precession field axis is determined by the ratio of the currents in the two coils, and the sizes of the fields determine the angle φ of the precession. The orientation of the polarization vector can therefore be defined in any direction.

In order to produce a continuous rotation of the polarization, *i.e.* a well defined precession, as required in neutron spin-echo (NSE) applications, precession coils are used. In the simplest case, these are long solenoids where the change of the field integral over the cross section can be corrected by Fresnel coils (Mezei, 1972). More recently, Zeyen & Rem (1996) have developed and implemented optimal field-shape (OFS) coils. The field in these coils follows a cosine squared shape that results from the optimization of the line integral homogeneity. The OFS coils can be wound over a very small diameter, thereby reducing stray fields drastically.

4.4.2.7.3. *Flipping of the polarization direction*

The term 'flipping' was originally applied to the situation where the beam polarization direction is reversed with respect to a guide field, *i.e.* it describes a transition of the polarization direction from parallel to antiparallel to the guide field and *vice versa*. A device that produces this 180° rotation is called a π flipper. A $\pi/2$ flipper, as the name suggests, produces a 90° rotation and is normally used to initiate precession by turning the polarization at 90° to the guide field.

The most direct wavelength-independent way of producing such a transition is again a non-adiabatic fast passage from the region of one field direction to the region of the other field direction. This can be realized by a current sheet like the Dabbs foil (Dabbs, Roberts & Bernstein, 1955), a Kjeller eight (Abrahams, Steinsvoll, Bongaarts & De Lange, 1962) or a cryoflipper (Forsyth, 1979).

Alternatively, a spin flip can be produced using a precession coil, as described above, in which the polarization direction makes a precession of just π about a direction orthogonal to the guide field direction (Mezei, 1972). Normally, two orthogonally wound coils are used, where the second, correction, coil serves to compensate the guide field in the interior of the precession coil. Such a flipper is wavelength dependent and can be easily tuned by varying the currents in the coils.

Another group of flippers uses the non-adiabatic transition through a well defined region of zero field. Examples of this type of flipper are the two-coil flipper of Drabkin, Zabidarov, Kasman & Okorokov (1969) and the line-shape flipper of Korneev & Kudriashov (1981).

references